Journal Name

ARTICLE TYPE

Cite this: DOI: 10.1039/xxxxxxxxxx

How are molecular crowding and the spatial organization of a biopolymer interrelated†

Chanil Jeon,[a] Changbong Hyeon,*[b] Youngkyun Jung,*[c] and Bae-Yeun Ha*[ab]

Received Date
Accepted Date

DOI: 10.1039/xxxxxxxxxx

www.rsc.org/journalname

In a crowded cellular interior, dissolved biomolecules or crowders exert excluded volume effects on other biomolecules, which in turn control various processes including protein aggregation and chromosome organization. As a result of these effects, a long chain molecule can be phase-separated into a condensed state, redistributing the surrounding crowders. Using computer simulations and a theoretical approach, we study the interrelationship between molecular crowding and chain organization. In a parameter space of biological relevance, the distributions of monomers and crowders follow a simple relationship: the sum of their volume fractions rescaled by their size remains constant. Beyond a physical picture of molecular crowding it offers, this finding explains a few key features of what has been known about chromosome organization in an *E. coli* cell.

1 Introduction

Cell's interiors are crowded with dissolved biomolecules such as proteins and RNA, which are abundantly present – to the extent that the typical distance between neighboring proteins is comparable to their size[1–4], as well perceived artistically[2,5]. They compete for space and thus exert excluded volume effects on other molecules. The resulting crowding effects, leading to non-ideal solution behavior[6], control various processes including protein folding/aggregation and chromosome organization/compaction[7–11] as well as gene regulation and cell growth[1–3,10]. A key concept is the entropic (depletion) force between monomeric units, oligomers, or biomolecular complexes[12,13]. Indeed, it has been shown to be a major determinant of chromosome organization in a bacterial cell[7,14–16]. If this entropic effect is modest for protein folding[17,18], it becomes increasingly important for the association of larger protein aggregates or biomolecular complexes[8].

Of particular interest is how molecular crowding controls the global vs. local organization of bacterial chromosomes in such a way to benefit other processes, especially transcription and cell growth[10,11] (see also Refs.[19–22]). While the chromosome is overall compacted by molecular crowding, transcription-active sites will experience stronger crowding effects as schematically shown in Fig. 1 (see also Ref.[12] for a physical basis); during fast growth, this is responsible for the clustering of these sites into the so-called 'transcription foci'[10,11].

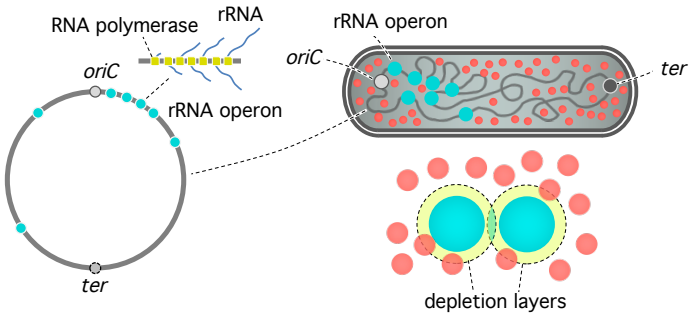

Fig. 1 Schematics of the *E. coli* chromosome. Ribosomal RNA (rRNA) operons (big spheres in cyan) are mostly concentrated near *oriC*. Molecular crowding can influence both the global and local organization of a heterogeneous polymer such as the *E. coli* chromosome. For simplicity, possible topological complexities (e.g., multi-fork or "branched-donut"[28]) are not shown. Overlapping of depletion layers (dashed spheres) leads to an entropic gain of crowders.

The key to understanding molecular crowding as for chromosome organization is a systematic treatment of both monomers and crowders. Indeed, both species exert volume-exclusion effects on each other; what is important is the interplay between their spatial distributions. How are then monomers and crowders distributed or how are their distributions interrelated? Does there exist a general relation for the spatial distributions of monomers and crowders? Despite much renewed interest and despite its relevance for bacterial chromosome organization[17,23–27], these basic questions have remained to be answered.

[a] *Department of Physics and Astronomy, University of Waterloo, Waterloo, Ontario, Canada N2L 3G1. E-mail: byha@uwaterloo.ca*
[b] *School of Computational Sciences, Korea Institute for Advanced Study, Seoul 02455, Korea. E-mail: hyeoncb@kias.re.kr*
[c] *Supercomputing Center, Korea Institute of Science and Technology Information, Daejeon, 34141, Korea. E-mail: yjung@kisti.re.kr*

† Electronic Supplementary Information (ESI) available: [details of any supplementary information available should be included here]. See DOI: 10.1039/b000000x/

Using molecular dynamics (MD) simulations and theoretical arguments, we offer a coherent view of molecular crowding and its impact on a long chain molecule formed by subunits or monomers. To this end, we establish a general relationship for the spatial distribution of monomers and crowders, referred to as a "density sum rule," which states that the sum of their volume fractions rescaled by their size remains constant. Even though it is primarily for a homogeneous polymer, it has nontrivial implications for the local and global organization of a heterogeneous polymer (e.g., clustering of large monomers), as illustrated in Fig. 1 (for simplicity, such topological complexities as multi-fork or "branched-donut"[28] are left out).

The bacterial chromosome is decorated with other molecules (e.g., RNA polymerases) and is heterogeneous in structure[9,19–22,29,30]. A simple but conceptually-meaningful model is a heterogeneous polymer consisting of big and small monomers confined in a crowded space, as illustrated in Fig. 1 (see Sec. 3 for details). Under the right conditions, the big monomers or transcription-active sites can cluster, as expected for the formation of transcription foci[10,11] (see Refs.[11,31] for similar entropic chromosome organization in eukaryotic cells). Molecular crowding has been considered to be responsible for this[10,11]. Using the density sum rule, we map out possible scenarios for the spatial organization of bacterial chromosomes. For instance, we clarify the condition under which big monomers can cluster by molecular crowding.

It is worth clarifying the scope of this work. We primarily focus our effort on characterizing a homogeneous polymer in a crowded space, especially in a parameter space of biological relevance. The so-called colloid limit, in which crowders are bigger than chain molecules, belongs to a distinct class of problems[13], and will not be considered here. Also we model both monomers and crowders as simple (structureless) hard spheres. For generality, we consider the two cases: $a > a_c$ and $a < a_c$, where a and a_c are the size or diameter of monomers and crowders, respectively *. The large-a case can be considered as a coarse-grained model of bacterial chromosomes, in which each monomer represents approximately a structural unit or topological domain[7,15,16,27], organized by various proteins[7,16]. Since each monomer contains many persistence lengths of DNA (~ 100kb long[7]), the notion of chain stiffness becomes much less relevant for the chromosome than for the DNA. The applicability of such a model can be tested in terms of the extent to which it serves its purpose. Indeed, similar coarse-grained models have been useful for gaining quantitative insights into a *large-scale* behavior of biomolecular systems (e.g., chromosome organization and segregation)[17,23–25,30,32]. On the other hand, the small-a case is relevant for protein or RNA folding[2–4,8].

On physics grounds, one may argue that the aforementioned heterogeneous model will likely combine both features of the large- and small-a cases (see Fig. 1). Thus, a homogeneous polymer not only merits much consideration on its own right but also offers guiding principles for understanding such a heterogeneous polymer.

Along this line, it is useful to note that in a biologically-relevant parameter space the way a flexible polymer responds to crowding is *intrinsically* generic and largely insensitive to confinement[18], in contrast to what was seen with DNA molecules[26]. As a result, the effects of crowding can be correctly mimicked by adjusting the excluded volume of monomers υ, which is the second virial coefficient of monomer interaction (see for instance Ref.[33]). Indeed, there exists a general relationship between υ and crowder's volume fraction ϕ_c, independently of confinement, as assumed in an effective-solvent picture. Confinement effects will not be reflected in local properties such as the density-sum rule derived in this paper. This may justify the neglect of confinement. Indeed it is shown in the Appendix that it remains applicable under slit-like confinement.

This paper is organized as follows. The simulation procedure is outlined in Sec. 2. Sec. 3 is devoted to the spatial organization of monomers and crowders; in particular, a density-sum rule is derived primarily based on simulation data and supplemented with theoretical arguments. It is then extrapolated to heterogeneous polymers for biophysical modelling of bacterial chromosomes.

2 Simulations

In our simulations, all particles (monomers and crowders) are assumed to be spherical, interacting with each other through the fully-repulsive Weeks-Chandler-Anderson (WCA) potential[35]:

$$U_{\rm WCA}(r) = \begin{cases} 4\varepsilon\left[\left(\frac{\sigma_{ij}}{r}\right)^{12} - \left(\frac{\sigma_{ij}}{r}\right)^{6} + \frac{1}{4}\right] & \text{for } r < 2^{1/6}\sigma_{ij} \\ 0 & \text{otherwise} \end{cases} . \quad (1)$$

Here, r is the center-to-center distance between particles; ε and σ_{ij} ($i = 1,2$) describe the strength and range of $U_{\rm WCA}(r)$; the subscripts i and j are used to distinguish between monomers and crowders: $\sigma_{11} = a$ (monomer size), $\sigma_{22} = a_c$ (crowder size), and $\sigma_{12} = (a + a_c)/2$ (i.e., the closest center-to-center distance between a monomer and a crowder.

Two adjacent monomers are held together via the finite extensible nonlinear elastic (FENE) potential[36,37]:

$$V_{\rm FENE}(r) = -\frac{1}{2}k_0 r_0^2 \ln\left[1 - \left(\frac{r}{r_0}\right)^2\right]. \quad (2)$$

The spring constant is set to $k_0 = 30\varepsilon/a^2$ and the range of the potential to $r_0 = 1.5a$. This is to ensure that the bond length is comparable to a with minimal bond-length fluctuations.

The velocity Verlet method is used to integrate the Newton's equation of motion[38]. The mass of the monomers and crowders is chosen as the mass unit. The units of length, energy, and time of our simulation are a, ε, and $\tau_0 = a\sqrt{m/\varepsilon}$, respectively. The simulation time step $\delta\tau$ is set to $0.002\tau_0$ for $a > a_c$ or $0.005\tau_0$ otherwise. The Langevin thermostat is employed with a damping constant $0.1\tau^{-1}$ to keep the temperature at $T = 1.0\varepsilon/k_B$, where k_B is Boltzmann constant[37]. (The choices of m and the damping

* Here the distinction between these two cases is based on our model: crowders and monomers as structureless hard spheres. The resulting size comparison scheme is not so conclusive for more realistic crowders and monomers. For instance, PEG (polyethylene glycol), often used in experiments as substitutes for the cytoplasmic crowders is a polymeric crowder[7]. In this case, the a-dependence of molecular crowding effects can be different[34].

constant are not important in our work because they do not affect equilibrium quantities.)

The entire system is enclosed in a cubic box of some large volume, typically as large as three times the chain size; periodic boundary conditions are imposed at the box surface in all directions (or in the directions parallel to the confining plates in the case of slit confinement).

Initially, the polymer is organized in a helical shape but crowders are distributed randomly. After chain equilibration, we run our simulation for 5×10^7 time steps and obtain data every $1,000$ steps. We repeat the entire simulation eight times with different random number seeds for Langevin thermostat as well as for initial crowder distributions. This is equivalent to preparing eight thermodynamically equivalent systems that evolve along distinct paths in the phase space. Ensemble averages are obtained as a time average within each run, which is then averaged over different simulations.

3 Spatial organization of monomers and crowders

3.1 Simulation results

We have calculated a number of quantities describing a polymer in a crowded space. Fig. 2 displays our results for the normalized chain size R/R_0 as well as the spatial distributions of monomers and crowders for the two cases: $a > a_c$ (A) and $a < a_c$ (B). (In the former case, each monomer may represent the structural unit of bacterial chromosomes[7,15,16,27], as illustrated on the top.) Here, a is the monomer size, a_c the crowder size, ϕ_c the volume fraction of crowders, R the chain size, and $R_0 = R(\phi_c = 0)$. † Also, ϕ_c is defined as the volume fraction of crowders at "infinity", i.e., somewhere inside the crowder-only region, where ϕ_c is constant. Let r be the distance from the center of mass of the polymer (not to be confused with r in $U_{\rm WCA}(r)$), then $\phi_c = \phi_c(r=\infty)$. ‡

For $a > a_c$ (A), we have chosen the number of monomers $N = 50$. If the radius of gyration is $R_g \approx 5a$, the Flory radius is $R_F \approx 1.1N^{3/5} \approx 12a$ (see for instance Ref.[39]). For $a < a_c \le 20a$ (B), a much lager $N = 2,000$ was used for an obvious reason: R_F has to be appreciably larger than a_c ($R_F \approx 105a$ for $N = 2,000$).

The R/R_0 graphs on the left in Fig. 2(A) and (B) show how molecular crowding collapses chain molecules, consistent with earlier results[17,18,23,24]. § These graphs also suggest that molecular crowding works differently between $a > a_c$ and $a < a_c$. It is the ratio $a\phi_c/a_c$ for $a > a_c$ but the single parameter ϕ_c for $a < a_c$ that controls R/R_0[18]. This has an interesting consequence on the ability of crowding to bring together two monomers. If $a > a_c$, the attraction between two monomers is stronger if they are larger (Fig. 3(A)). Otherwise, a distinct conclusion can be reached: their attraction is insensitive to a but is set by ϕ_c only (Fig. 3(B)), if $a_c > a$. The graph on the left in Fig. 2(B) suggests that the curve for $a_c = 20a$ is somewhat exceptional in that it appears to deviate from other curves for smaller a_c. For a large a_c value, the correlation between crowders are stronger. This may explain the deviation (see Refs.[17,18] and references therein for details).

Indeed, the observation above can be understood in terms of the (maximum) depletion-free energy gain[10,12]:

$$\frac{\Delta F_{\rm dep}}{k_BT} \approx \phi_c\left(1+\frac{3a}{2a_c}\right) + \mathcal{O}(\phi_c^2) \approx \begin{cases} \frac{3}{2}\frac{a\phi_c}{a_c}, & a > a_c \\ \phi_c, & a < a_c \end{cases} . \qquad (3)$$

This is well aligned with the view of crowding effects as reducing the solvent quality, thus diminishing the excluded volume of each monomer[18]: $\upsilon \approx \upsilon_0(1-\alpha\phi_c)$, where $\alpha = 3a/a_c$ for $a > a_c$ or $\alpha = 1$ otherwise, where υ_0 is the excluded volume when $\phi_c = 0$: $\upsilon_0 \approx a^3$ for WCA monomers. The scaling form of $F_{\rm dep}$ is consistent with the trend shown by the graphs of R/R_0 in Fig. 2.

A general picture emerging from our discussion above is that smaller crowders are "better" if $a > a_c$, confirming earlier results[4,10,12,18,23–25], or all are "equal" if $a < a_c$, for a given ϕ_c value (see Fig. 3(A) & (B))[18]. As a result, the degree of crowdedness is controlled by $a\phi_c/a_c$ for $a > a_c$ or ϕ_c for $a < a_c$. If applied to a heterogeneous polymer consisting of big and small monomers, the clustering tendency of big ones will be sensitive to a_c, i.e., smaller is better.

To further exploit crowding effects, possibly for a heterogeneous polymer, note that the depletion interaction between small and big monomers is also known[10]:

$$\begin{aligned} \frac{\Delta F_{\rm dep}(a_m, a_{\rm M})}{k_BT} &\approx \phi_c\left(1+\frac{3a_m a_{\rm M}}{a_c(a_m+a_{\rm M})}\right) \\ &\approx \phi_c\left(1+\frac{3a_m}{a_c}\right) \\ &\approx \begin{cases} 3\frac{a_m\phi_c}{a_c}, & a_m > a_c \\ \phi_c, & a_m < a_c \end{cases} . \end{aligned} \qquad (4)$$

The second equality follows from the inequality $a_{\rm M} \gg a_m$.

It is worth noting the parallelism between Eq. 4 and Eq. 3. The depletion interaction between small monomers or between small and large ones relies on ϕ_c, as long as $a_m < a_c$; it is controlled by the ratio $a_m\phi_c/a_c$ if $a_m > a_c$ (see Fig. 3(C) & (D)). The big size of big monomers is irrelevant for the interaction between big and small monomers. This implies that the interaction between big monomers can be much stronger than other interactions. It also allows us to extract useful information about a heterogeneous polymer from our understanding of corresponding homogeneous cases. This non-uniformity in depletion forces can govern the local organization of a heterogeneous polymer and induce clustering of big monomers under the right conditions, as schematically shown in Fig. 1.

The results in Fig. 2(B) suggest that for $a_c > a$ crowding has modest effects on chain size in the physiological range of $\phi_c \approx 0.3$ (see Ref.[18] for details). This holds for heterogeneous polymers as

† For R, one can choose the Flory radius R_F or the radius of gyration R_g. If $\mathbf{r}_n$ is the position vector of monomer n ($n = 1,2,...,N$) and $\mathbf{R}_{\rm CM} = \frac{1}{N}\sum_n \mathbf{r}_n$ is the position of its center of mass, $R_g^2 = \frac{1}{N}\sum_n (\mathbf{r}_n - \mathbf{R}_{\rm CM})^2$. However, the ratio R/R_0 is the same for R_F and R_g.

‡ For a practical purpose, ϕ_c defined this way is essentially identical to the average volume fraction of crowders, as long as the simulation box is large enough.

§ The origin of the slight non-monotonic dependence of R/R_0 on ϕ_c in Fig. 2(A) is not entirely clear[17,18,23,24]. Recently, it has been attributed to kinetic effects[23,24] (see Ref.[18] and references therein for alternative views).

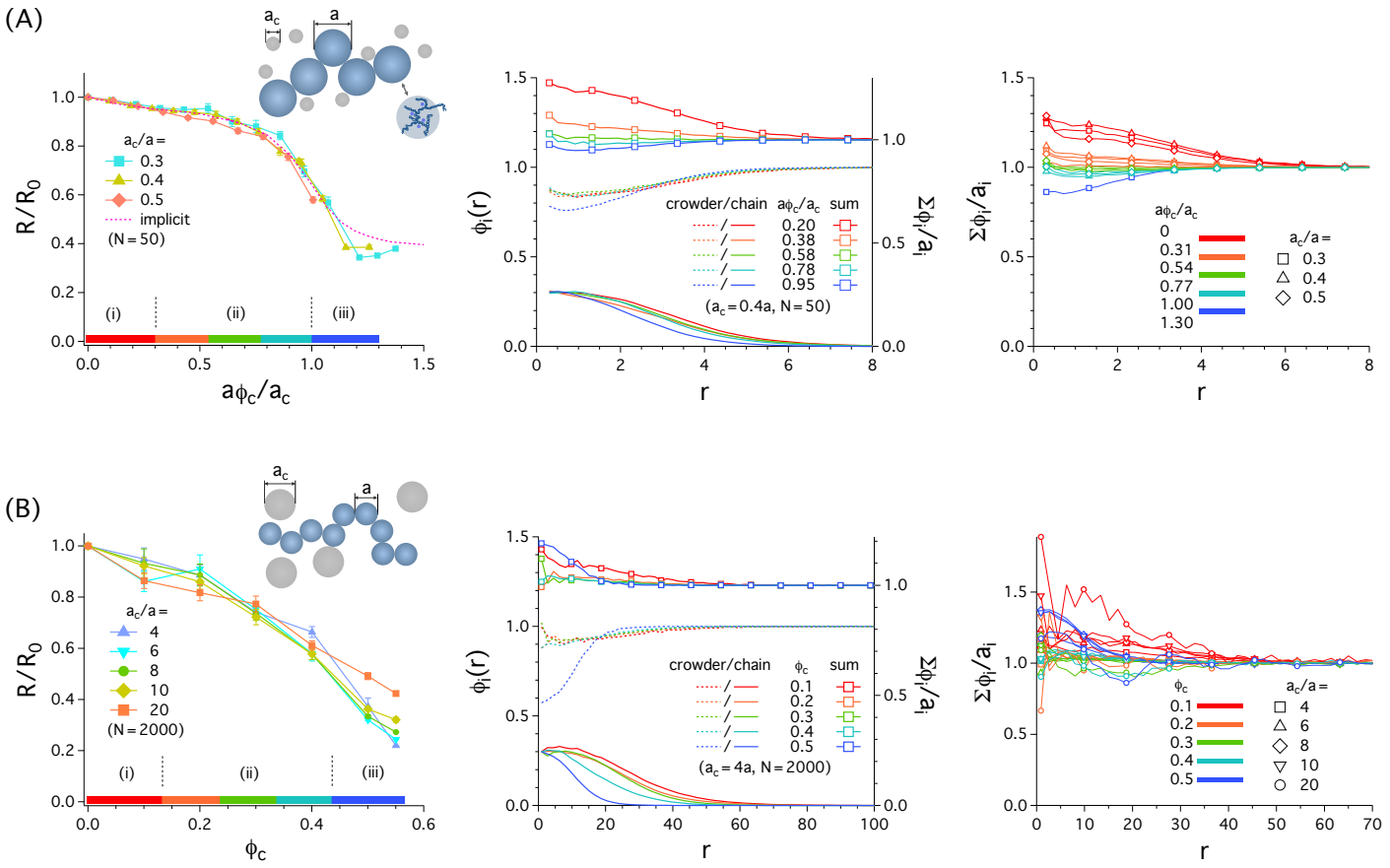

Fig. 2 Compaction of a polymer by molecular crowding (left column) and spatial distribution of monomers and crowders (middle and right columns). If the graphs in (A) represents the small-crowder case ($a > a_c$), those in (B) describe the large-crowder case ($a_c > a$). The simulation parameters used are $N = 50$ in (A) and $N = 2,000$ in (B); the sizes of crowders are $a_c = 0.3, 0.4, 0.5a$ (A) to $4, 6, ..., 20a$ (B). In the left graphs, the normalized chain size R/R_0 is plotted against the ratio $a\phi_c/a_c$ (A) or ϕ_c (B). Here R_0 is the equilibrium chain size in the absence of crowders and $\phi_c = \phi_c(r = \infty)$. For $a > a_c$, R/R_0 is a function of $a\phi_c/a_c$, whereas for $a_c > a$, it is controlled by ϕ_c alone. Also superimposed is the corresponding effective-solvent result (dashed line in magenta) originally reported in Ref.[18], in which a relationship between ϕ_c and the effective excluded volume υ was obtained by mapping the explicit-crowder case onto one in which the effects of crowders are mimicked by reducing υ. The varying degrees of compaction is represented by the color bar on the x axis: weak (i), moderate (ii), and strong (iii); the color bar matches the color scheme used in all other graphs in (A) and (B). The middle graph in both (A) and (B) shows the volume fraction $\phi_i(r)$ of monomers and crowders with $i =$ 'm' (monomer) or 'c' (crowder), plotted on the left axis, as well as $\sum_i \phi_i(r)/a_i$ on the right axis, for $a_c = 0.4a$ (A) and $a_c = 4.0a$ (B); also note that r is the longitudinal distance from the center of mass of the polymer. For visual clarity, $\phi_c(r)$ is normalized as $\phi_c(r)/\phi_c(r = \infty)$ and $\phi_m(r)$ as $\phi_m(r)/\phi_m(r = 0)$; $\sum_i \phi_i(r)/a_i$ is rescaled by $\sum_i \phi_i(r = \infty)/a_i$. The results in this graph suggest coexistence of monomer-rich and crowder-rich phases. When the polymer is moderately compacted (ii), $\sum_i \phi_i(r)/a_i$ tends to a constant through the entire range of r shown and converges onto $\phi_c(r = \infty)/a_c$. The graph on the right in both (A) and (B) summarizes the results for $\sum_i \phi_i(r)/a_i$ for various choices of a_c. In regime (ii), $\sum_i \phi_i(r)/a_i \approx \phi_c(r = \infty)/a_c$ is satisfied for all a_c values used, possibly except for $a_c = 20a$ in (B); the more pronounced deviation for $a_c = 20a$ can be attributed to stronger positional correlations among crowders. Possibly except for this case, outside regime (ii), $\sum_i \phi(r)/a_i$ deviates from $\sum_i \phi_i(r = \infty)/a_i$ by about 15% at most (at $r \simeq 0$). (Error bars are shown for a few representative curves.)

well, as long as the "big monomers" are smaller than crowders, as suggested by Eq. 4. A good example is intrinsically disordered proteins (IDPs) (see Ref.[17] and relevant references therein). The complexity of IDPs would not necessarily invalidate our finding based on a polymer model; their internal structure will make the proteins more heterogeneous but they still belong to the case $a_c > a$. However, crowding effects become more important between protein oligomers and aggregates[8,18], as indicated by Eq. 3 for the case $a > a_c$.

Earlier, we have shown that the scaling behavior of R as a function of ϕ_c depends on how crowders are assumed to be distributed[18]. For instance, the simulation results for R are consistent with the picture that the chain-occupying region is permeable to crowders. How are monomers and crowders actually distributed in the presence or absence of confinement? In a homogeneous system consisting of crowders only, the density of crowders tends to be uniform. In a mixture of small and large particles, however, large particles tend to get phase-separated from small ones[13]. Monomers on a chain molecule can be similarly organized in a crowded medium. In both cases, the uniform density picture does not hold any longer. What kind of rule governs their distribution?

Fig. 2 also shows how chain compaction is related to the spatial organization of monomers and crowders (middle and right graphs). In the graph of R/R_0 on the left in Fig. 2, we depict a varying degree of compaction: weak (i), moderate (ii), and strong (iii). The distinction between the regimes is inspired by the graphs in the middle column in Fig. 2, as evidenced below. Furthermore, the color bar on the x-axis matches the color scheme used in the other two graphs.

The graph in the middle in Fig. 2(A) shows the volume fraction $\phi_i(r)$ of monomers and crowders (left axis) as well as $\sum_i \phi_i(r)/a_i$ (right axis) for $a_c = 0.4a$, where with $i =$ 'm' (monomers) or 'c' (crowders); recall r is the radial distance from the center of mass of the polymer. Obviously, $a_m = a$ and ϕ_m is the volume fraction of monomers. In this expression and related ones below, a is shown explicitly. For visual clarity, $\phi_c(r)$ is normalized as $\phi_c(r)/\phi_c(r=\infty)$ and $\phi_m(r)$ as $\phi_m(r)/\phi_m(r=0)$; $\sum_i \phi_i(r)/a_i$ is rescaled by $\sum_i \phi_i(r=\infty)/a_i$. The results in this graph suggest coexistence of monomer-rich and crowder-rich phases separated by a rather smooth boundary.

When the polymer is moderately (ii) or strongly compacted (iii), $\sum_i \phi_i(r)/a_i$ tends to a constant through the entire range of r shown and converges onto ϕ_c/a_c; recall that $\phi_c = \phi_c(r=\infty)$ is the value of $\phi_c(r)$ somewhere deep inside the crowder-only region. This can be summarized as

$$\sum_i \frac{\phi_i(r)}{a_i} \approx \frac{\phi_c}{a_c} \tag{5}$$

or

$$\sum_i a_i^2 \rho_i(r) \approx a_c^2 \rho_c, \tag{6}$$

where $\rho_i \approx \phi_i/a_i^3$ is the density of monomers ($i =$ m) or crowders ($i =$ c). Hereafter, Eq. 5 is referred to as the "sum rule" for ϕ_i and Eq. 6 as the "density-sum rule" or "density-sum equality"; since Eqs. 5 and 6 are equivalent, they will be called the density-sum rule for simplicity. ¶

We have also used a few choices of a_c and plotted our results for $\sum_i \phi_i(r)/a_i$ in Fig. 2(A) (right). When the polymer is moderately compacted, the equality in Eq. 5 is satisfied for all a_c values used ((ii) is a regime of biological relevance, where the equality holds well); $\sum_i \phi_i/a_i$ is nearly constant for the entire range of r. When it is strongly compacted, $\sum_i \phi_i/a_i$ deviates from a constant a bit more appreciably for $a_c = 0.3a$, but the deviation is insignificant, i.e., about 15% at most at $r = 0$.

An earlier study shows that in a poly(bi)-disperse crowded medium R/R_0 is a function of $\sum_c a\phi_c/a_c$ only for a given N value, if $a > a_c$ is assumed, where the sum is over all crowder types: small and large. This suggests that the relation in Eq. 5 can be extrapolated to the poly-disperse case as

$$\frac{\phi_m(r)}{a} + \sum_c \frac{\phi_c(r)}{a_c} \approx \sum_c \frac{\phi_c}{a_c}. \tag{7}$$

In Fig. 2(B) (middle and right graphs), we have extended the sum rule in Eq. 5, i.e., $\sum_i \phi_i(r)/a_i \approx \phi_c/a_c$, established for $a > a_c$, to the case $a < a_c$. First note that it is the ratio ϕ_i/a_i ($i =$ c or m) that enters into this relation. As a result, the left hand side remains invariant under the exchange in role between 'c' and 'm.' This suggests that this relation may as well hold for $a < a_c$, as long as a_c is not too large. For the highly asymmetric case $a_c \gg a$, however, our polymer-crowder system appears to belong to a distinct class of problems, as also suggested by the results for R/R_0 in Fig. 2(B) (see Ref.[18] for additional details). In this case, the spatial ordering among crowders becomes important at a high-ϕ_c range (see Ref.[17] and references therein). As a result, the aforementioned invariance will not have to be preserved.

The middle and right graphs in Fig. 2(B) display our results for ϕ_i as well as $\sum_i \phi_i/a_i$ for the case $a_c > a$, obtained for $N = 2{,}000$ and for several values of ϕ_c, including a physiologically relevant range. (Middle) For $a_c = 4a$, the sum rule in Eq. 5 (i.e., $\sum_i \phi_i(r)/a_i \approx \phi_c/a_c$) holds well, almost perfectly for $\phi_c \approx 0.3$. (Right) This graph compares various choices of a_c: $a_c = 4, \ldots, 20a$. The sum rule holds better for $a_c = 4a, 6a$ than for $a_c = 20a$. Especially for $\phi_c = 0.3$, it works nearly perfectly for $a_c = 4a, 6a$, similarly to the case $a < a_c$ in Fig. 2(A).

The density-sum rule can be used for different purposes. First, it gives a physical sense of full compaction that occurs at $a\phi_c/a_c \approx 1$. Under this condition, Eq. 5 becomes $\phi_m(r) + a\phi_c(r)/a_c \approx 1$. Unless the chain is maximally or closely compacted, i.e., $\phi_m \approx 1$, $\phi_c \neq 0$. This means that the chain-occupying region is still permeable to crowders.

Indeed, the main advantage of our analysis based on the sum rule in Eqs. 5-7 is that it is a thermodynamic relation, in which the entropy of crowders and monomers is captured simultaneously at least approximately in a biologically-relevant parameter space. This picture is thermodynamically more meaningful than a two-body picture, in which the depletion force between two

¶ Since $\rho_m = \rho_m(r=\infty) = 0$, Eq. 6, for instance, can be rewritten in a more symmetric form $\sum_i a_i^2 \rho_i(r) \approx \sum_i a_i^2 \rho_i$. This can be correctly called a (rescaled) density-sum equality.

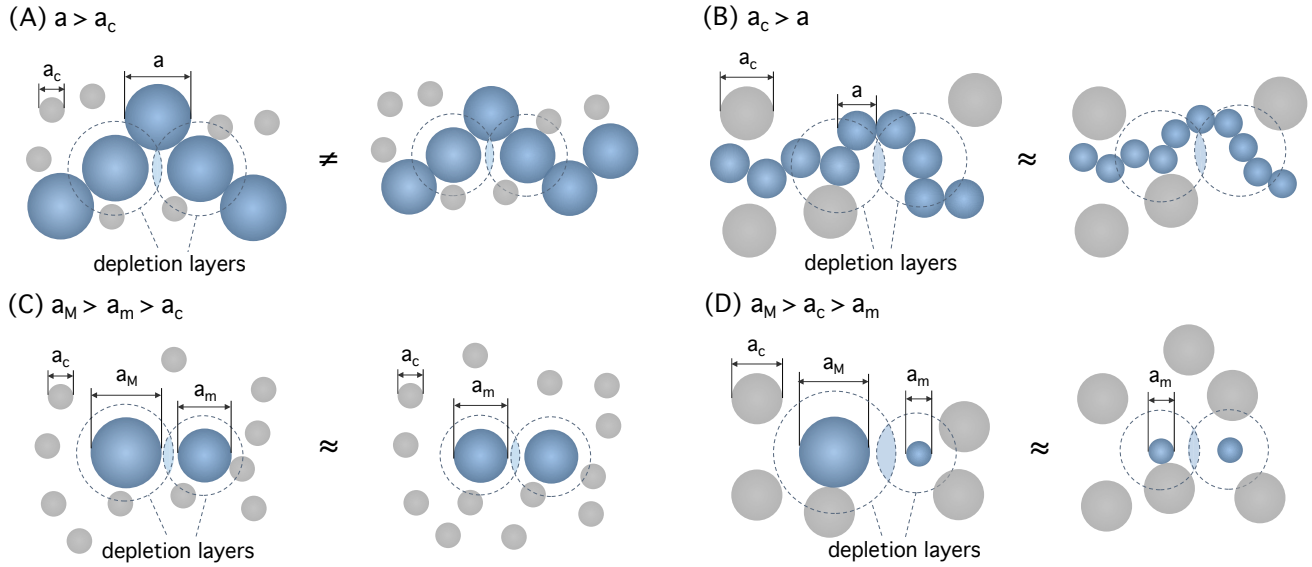

Fig. 3 Analysis of the "quality" of crowders for a homogeneous ((A) & (B)) or heterogeneous polymer ((C) & (D)). Recall that a is the monomer size and a_c the crowder size. In all cases, crowders exert excluded-volume effects against each other and on the polymer they surround, inducing depletion forces between monomers. (A) For $a > a_c$, the depletion force is obviously stronger if a is larger, because of a larger overlapped (shaded) region. This is equivalent to saying that smaller crowders are better for a given ϕ_c value. (B) When $a_c > a$, the depletion force is independent of a for a fixed ϕ_c value. In this case, the volume of the depletion layer is mainly determined by a_c, independently of a, and all crowders are equal. (C) & (D) Depletion forces in a heterogeneous chain. Two cases are contrasted: $a_{\rm M} > a_{\rm m} > a_c$ (C) and $a_{\rm M} > a_c > a_{\rm m}$ (D). In both cases, the depletion force between big and small monomers is set by the size of the small one. If it depends on $a\phi_c/a_c$ in (C), it is controlled by ϕ_c alone in (D). If smaller crowders are better in (C), all are equal in (D); the effect of crowding is modest in (D), similar to what is shown in (B). This implies that the depletion forces between monomers in a heterogeneous polymer can be reduced to those in the corresponding homogeneous polymers as shown in (A) & (B); the former combines both features of (A) & (B).

monomers is focused on (see Eq. 3). Furthermore, Eq. 7 or its variation can find relevance for chromosome organization as discussed below.

3.2 Free energy analysis

Considering its simplicity, the sum rule in Eq. 5 merits theoretical consideration. A binary mixture of hard spheres (whether strung or unstrung) is only deceptively simple but offers a rich source of problems for statistical physics [13,41]. Here we present a simple but physics-oriented approach, focusing on regime (ii) beyond the onset of chain compaction. In regime (ii), chain connectivity may not play an important role. Here crowders will be treated as reducing the solvent quality, diminishing υ from $\upsilon_0 \approx a^3$ to a negative value [18]. This enables us to adopt a free-energy approach developed for a mono-disperse hard sphere system in solution [42,43]. Using this, we derive the spatial distribution of monomers and crowers across the phase boundary. To this end, we implement the conventional picture, in which a sharp phase boundary is assumed [42,43].

Here, we use a standard lattice model of a symmetric solution, in which each site is occupied by either solute or solvent molecule [42,43]. Our intention is to present Eq. 5 in a thermodynamic context. Let a be the lattice constant, $\Delta\varepsilon$ the effective interaction between solute molecules, ϕ the volume fraction of solute molecules, and χ the usual parameter describing the degree of miscibility, which scales as $\chi \sim -\Delta\varepsilon/k_BT$; by convention, $\Delta\varepsilon < 0$ if monomers attract each other. If a sharp phase boundary is assumed, one arrives at the coexistence-curve equation [42,43]:

$$\chi = \frac{1}{1-2\phi}\ln\left(\frac{1-\phi}{\phi}\right). \tag{8}$$

As it is, this relation does not give useful information about the "shape" of the phase boundary. To exploit it beyond its original scope, let us picture the boundary as consisting of multiple layers; inside each layer located at r (the center of a solute-rich phase is at $r = 0$), ϕ is constant. Let $\delta\phi$ be the variation of ϕ between the two consecutive layers and $\delta\chi$ the corresponding χ change: $\delta\chi \sim \delta\Delta\varepsilon/k_BT \sim -a\delta\phi_c/a_c$ for the case $a > a_c$. The sign change in the first equality is to reflect the fact that χ decreases as r increases. Well above the phase separation point, one can show from Eq. 8 that $\delta\chi \sim \delta\phi$ or $-a\delta\phi_c/a_c \sim \delta\phi$. By integrating this from infinity to a target position r, we arrive at

$$-a\int_\infty^r \frac{\delta\phi_c}{a_c} \sim \int_\infty^r \delta\phi \quad \rightarrow \quad -\frac{\phi_c(r)}{a_c} + \frac{\phi_c(r=\infty)}{a_c} = \frac{\phi(r)}{a}. \tag{9}$$

In the last equality, we assumed that $\phi(\infty) = 0$, as expected for a single chain molecule of finite N. The relation in Eq. 9 is equivalent to Eq. 5, which holds well if the chain is moderately compressed (see Fig. 2).

In the analysis above, the size of monomers coincides with the lattice constant but the size of crowders is implicitly taken into account via χ. In this regard, it is better suited for the case $a > a_c$.

For the other case $a_c > a$, we content ourselves by recalling the symmetry argument described below Eq. 7.

What is the role of chain connectivity, which was left out in our consideration, in addition to ensuring that $\phi(r=\infty)=0$? This effect is expected to be marginal well above the onset of a phase separation. Indeed, it has been shown numerically that a binary mixture of hard spheres satisfies a similar density sum rule [44].

3.3 Applications to a heterogeneous polymer

Our analysis in Fig. 3(C) & (D) suggests that a simple physical picture may be mapped out for a heterogeneous polymer, as is most obvious if (D) is assumed. The clustering of big monomers is then reduced to a multi-loop problem, in which the intervening sections are assumed to be uninfluenced appreciably by crowding [10]. In this picture, the depletion interactions between big monomers compete with the entropic penalty of looping.

As noted at the end of subsect. 3, the sum rule in Eq. 5 or its variation can offer a thermodynamically-consistent picture. In this subsection, we map out possible scenarios for clustering based on the sum rule.

If chain connectivity were ignored, it would be tempting to extrapolate Eq. 7 to a heterogeneous polymer, consisting of big and small monomers, as

$$\frac{\phi_{\rm M}(r)}{a_{\rm M}}+\frac{\phi_m(r)}{a_m}+\sum_c\frac{\phi_c(r)}{a_c}\approx\sum_c\frac{\phi_c}{a_c}, \tag{10}$$

where the subscript 'M' refers to large monomers and 'm' to small ones. Here, monomers (both big and small) and crowders are treated on an equal footing in this expression, similarly to what Eq. 5 or Eq. 7 indicates. In other words, the terms on the left hand side of Eq. 10 are symmetrical between monomers and crowders. However, there is a subtle difference between homogeneous and heterogeneous chains.

Association of two big monomers in the heterogeneous case occurs at the expense of chain entropy, similarly to what we would expect from polymer looping [10,45]. As a result, the spatial distribution of a heterogeneous polymer depends on the contour position of big monomers. In other words, such a polymer will not necessarily satisfy a general rule for monomer/crowder distributions. A related point is that confinement will influence the spatial positioning of big monomers and looping as well. Considering this complexity, simplification is not only inevitable but also helps us develop guiding principles for understanding a more realistic case. Indeed, if used with caution, Eq. 10 provides useful insights into the spatial organization of a heterogeneous chain. For instance, it will offer a lower bound for $a_{\rm M}$ required for the clustering of big monomers. Also it clarifies the biological picture of clustering, as evidenced below.

For any cluster of big monomers, $\phi_{\rm M}\approx 1$. If combined with Eq. 10, this leads to

$$\frac{\phi_{\rm M}}{a_{\rm M}}\approx\frac{1}{a_{\rm M}}\approx\frac{\phi_m(r)}{a_m}+\frac{\phi_c(r)}{a_c}\approx\frac{\phi_c}{a_c}. \tag{11}$$

The size requirement for the clustering of large monomers reads

$$a_{\rm M}\geq a_c/\phi_c. \tag{12}$$

Note that this condition is essentially identical to the full-compaction condition for a homogeneous polymer consisting of big monomers of size $a_{\rm M}$ only. Obviously, small monomers will experience weaker depletion forces, as illustrated in Fig. 3(C) & (D). For the case depicted in Fig. 3(C) & (D), depletion forces are weak between small monomers or between big and small monomers. Accordingly, there should exist a range of ϕ_c over which only big ones can cluster.

The heterogeneous polymer discussed above can be viewed as a simple but conceptually-meaningful model of the *E. coli* chromosome as a representative bacterial chromosome, as schematically shown in Fig. 1. A key determinant of chain heterogeneity is the binding of RNA polymerases (RNAPs) onto ribosomal RNA (rRNA) operons [10,21,22,46,47]. At slow growth rates, each rRNA operon is decorated with four 10 nm RNA polymerases. In contrast, in a fast-growing *E. coli* cell, each rRNA operon carries about seventy 10 nm RNA polymerases closely packed along the chromosome, making about one rRNA/85bp [46,47]. ‖ A somewhat larger value of a RNAP ($\approx$ 15 nm) was also used in the literature [48]. This difference, however, will not change our picture of clustering, as evidenced below. The big monomers can thus be viewed as representing ribosomal RNA (rRNA) operons or sections of the chromosome covered with RNAPs. Indeed, molecular crowding has emerged as a main driving force for the clustering of big monomers into transcription foci, in which transcription machineries are concentrated [10].

For a typical *E. coli* cell, $a_c \approx$ 5-7 nm and $\phi_c \approx 0.3$ [2,49,50]. Eq. 12 then reads $a_{\rm M} \geq$ 5-7 nm/0.3 $\approx$ 20 nm (corresponding to $F_{\rm dep} \approx 2k_BT$). Monomers smaller than this will not cluster. This implies that clustering in an *E. coli* cell needs to be considered "collectively." To see this, consider a hypothetical chain of thickness $a_{\rm M}$, chosen to be comparable to the size of RNA polymerase: $a_{\rm M} \approx$ 10 nm (or $a_{\rm M} \approx$ 15 nm). This does not satisfy the size requirement for clustering. If taken literally, our homogeneous chain analysis implies that transcription-active sites will not cluster. This appears to contradict the evidence of clustering under fast (but not slow) growth conditions [10,46,47].

We believe that this seeming contradiction can be resolved by clarifying the biological picture of clustering. Even though clustering will not occur at the level of individual RNAPs, *clusters* of RNAPs collectively can cluster into a bigger one; each cluster corresponds to an operon. In our model, these clusters can be coarse-grained into big monomers. The free energy gain of clustering between big monomers will depend on coarse-graining details [10]. At fast growth rates, in each operon, seventy 10 nm RNAPs are tightly packed: about one RNAP/85 base pairs [10] (also see

‖ In our consideration here, other details such as Christmas-tree-like structures formed by RNA molecules being made are ignored [46,47]. It is not entirely clear if these structures induce steric repulsions or enhance depletion forces by effectively increasing $a_{\rm M}$. An explicit consideration of their role is computationally demanding and will be left for future work.

Refs.[46,47]). This cluster can be coarse-grained into a big sphere of diameter $2\times 70^{1/3}\times 5\,\mathrm{nm}\approx 41\,\mathrm{nm}$. ** This value is above the required value for clustering, more so if RNAPs are assumed to be bigger. Literally speaking, a homogeneous chain consisting of monomers larger than this value will be fully compacted. This hard-sphere picture, however, tends to underestimate the depletion free energy gain ΔF_{dep}. If RNAP exchange/rearrangement between operons in close proximity is allowed, big monomers can be considered as "soft" in the sense that two can merge into one with a larger size $a_{\mathrm{M}}^{\mathrm{new}}=2^{1/3}a_{\mathrm{M}}$[10]. In our notation, the 'soft' depletion free energy becomes[10]

$$\frac{\Delta F_{\mathrm{dep}}}{k_BT}\approx\phi_c\left[\frac{2\left(a_{\mathrm{M}}+a_c\right)^3-\left(2^{1/3}a_{\mathrm{M}}+a_c\right)^3}{a_c^3}\right]. \qquad (13)$$

If we use $\phi_c=0.3$ and $a_c=7\,\mathrm{nm}$ together with $a_{\mathrm{M}}=41\,\mathrm{nm}$, we arrive at $\Delta F_{\mathrm{dep}}\approx 17\,k_BT$; using $a_c=5\,\mathrm{nm}$ will lead to a larger free energy $\approx 31\,k_BT$. These values are much larger than what one would expect from the hard-sphere picture, which results in several k_BT's. While the former values are comparable to or larger than the estimated free-energy cost for looping $\approx 17\,k_BT$[10] ††, the latter is much smaller than the looping free energy[10]. This suggests that clustering should be understood as a collective phenomenon.

The soft-sphere picture is not applicable to chromosomes in a slowly-growing cell, since RNAPs are much more sparsely distributed: four RNAPs per operon[10]. As noted above, even a chain uniformly decorated with RNAPs does not satisfy the clustering condition. Neither does the inhomogeneous chain mimicking the *E. coli* chromosome.

In summary, at fast-growth rates, transcription-active sites along the *E. coli* chromosome can occur 'collectively,' not at the individual RNAP level. This finding complements the earlier analysis of clustering[10], which clarifies the competition between crowding and looping. In contrast, at slow growth rates, their depletion attraction will not overcome the chain-entropy penalty for clustering. In this case, we have shown that the chromosome does not even satisfy the necessary condition for clustering in Eq. 12.

As a closing remark, we wish to mention that confinement will not easily modify our conclusion on clustering. In the Appendix, we have shown that the sum rule in Eq. 5 is satisfied in a confined space: (quasi) two-dimensional slit-like. In this sense, the sum-rule is a universal relation, which holds for both $a>a_c$ and $a_c>a$, independently of confinement.

** Here, we assume that RNAPs are closely packed. More realistically, one can include DNA segments that intervene the two adjacent RNPAs as well as rRNAs, and view each cluster as loosely packed RNAPs together with the intervening DNA and rRNAs[48]. This will change the depletion free energy gain for clustering F_{dep}. In this case, F_{dep} cannot be determined uniquely but will depend on whether the cluster is assumed to be permeable to crowders. In our consideration, we focus on the simpler view: each cluster is closely packed.

†† This represents looping in an unconfined space. Confinement can influence looping. In particular, cylindrical confinement reorganizes a chain molecule and thus modifies looping tendency.

4 conclusions

In conclusion, we have presented a unified picture of biomolecular crowding, in which chain/monomer sizes and the spatial distributions of monomers and crowders are interrelated. In particular, the interrelationship between the distributions of monomers and crowders is expressed in a simple form, referred to as the density-sum rule: $\phi(r)/a+\phi_c(r)/a_c\approx\phi_c^{\infty}/a_c$. According to this, the sum of the volume fractions of monomers and crowders rescaled by their size is constant. For the biologically-relevant ϕ_c range, this is accurate and holds generally, i.e., independently of other details (e.g., crowder sizes or confinement). Because of its simplicity and generality, this relationship will be useful for interpreting crowding effects in a cell-like crowded medium.

As a first step toward understanding a heterogeneous polymer, consisting of small and big monomers, we have analyzed the 'quality' of crowders. If monomers are larger than crowders, smaller crowders are better, for a given ϕ_c value. For the case of a heterogeneous polymer, the size dependence is more intriguing. The depletion force between big and small monomers is set by the small one in the sense that it is identical to the depletion force between small ones, irrespective of a_c, as illustrated in Fig. 3(C) and (D). As a result, if the smaller monomer is larger than crowders, smaller crowders are better; in contrast, if the smaller one is smaller than crowders, all crowders are equal. In the latter case, the depletion force is relatively weak for a biologically-relevant ϕ_c range[18].

According to the crowder-size analysis above (see Eq. 5 and Fig. 5), crowding has modest effects on the structure of intrinsically-disordered (coil-like) proteins[17]. Their molecular complexities such as secondary structures will not invalidate this prediction, since they still fall in the small-a case. Crowding effects become increasingly important for protein-protein interactions and association of protein aggregates[8].

A general picture emerging from this consideration is that the degree of compaction by molecular crowding is nonuniform for a heterogeneous polymer, more so if the degree of heterogeneity is larger. This is well aligned with the observation that the local vs. global compaction of bacterial chromosomes can be controlled by molecular crowding in concert with other processes such as transcription by ribosomal RNA polymerases[10,46,47]. This is responsible for the clustering of big monomers under the right conditions. Finally, the physical picture in Fig. 3(C) and (D), as also summarized above, implies that depletion forces in a heterogeneous polymer can reduce to those in the corresponding homogeneous cases. This may justify our clustering considerations, primarily based on a homogeneous polymer model.

Indeed, a heterogeneous polymer can be considered as a coarse-grained model of bacterial chromosomes organized with various proteins. A dominant source for chain heterogeneity is rRNA polymerases concentrated in several designated sites along the chromosome, i.e., rRNA operons[10,19–22,46,47]. At the crudest but non-trivial level, chain heterogeneity can be mimicked by introducing small and big monomers with the latter representing transcription-active sites (see Fig. 1)[10].

The density-sum rule in Eq. 10, in particular, has been useful

for understanding the local vs. global organization of such a heterogeneous polymer. For instance, it not only offered a necessary condition for the clustering of big monomers but also refined the biological picture of clustering. With typical parameters relevant for an *E. coli* cell, the necessary condition or the size requirement for clustering reads $a_{\mathrm{M}} \approx a_c/\phi_c^{\infty} \approx 20\,\mathrm{nm}$ (recall that the subscript 'M' refers to big monomers). Indeed, our analysis based on this is consistent with what has been known about the *E. coli* chromosome, which is organized differently under different growth rates[10,19–22,46,47]. It suggests that clustering can occur between 'clusters' of RNA polymerases (i.e., those in each operon), not between individual polymerases, since they individually do not satisfy the size requirement for clustering. As a result, clustering will not be induced by molecular crowding in *E. coli* chromosomes at slow-growth rates. In contrast, at fast-growth rates, the cluster of RNA polymerases (in each operon) satisfies the size requirement. Furthermore, theoretical arguments showed that the depletion force between the 'soft' clusters is strong enough for their clustering into transcription foci[10]. For a better understanding of clustering, an explicit consideration of a heterogeneous polymer in a confined space, crowded with poly-disperse crowders, will be desirable.

5 Acknowledgements

We acknowledge helpful discussions with S. Jun, M. Scott, and L. Liu. This work was supported by NSERC (Canada), the collaborative research contract funded by Korea Institute of Science and Technology Information (KISTI), and the Basic Science Research Program through the grant No. 2015R1D1A1A09057469 (YJ) as well as by KIAS (Korea Institute for Advanced Study). We acknowledge the computational resources of the Shared Hierarchical Academic Research Computing Network (SHARCNET: www.sharcnet.ca) and Compute/ Calcul Canada.

References

1 S. B. Zimmerman and A. P. Minton, "Macromolecular Crowding: Biochemical, Biophysical, and Physiological Consequences," *Annu. Rev. Biophys. Biomol. Struct.*, 1993, **22**, 27-65.

2 R. J. Ellis, "Macromolecular crowding: obvious but underappreciated," *Trends Biochem. Sci.*, 2001, **26**, 597-604.

3 H.-X. Zhou, G. Rivas, and A. P. Minton, "Macromolecular Crowding and Confinement: Biochemical, Biophysical, and Potential Physiological Consequences," *Ann. Rev. of Biophys.*, 2008, **37**, 375-397.

4 K. A. Sharp, "Unpacking the origins of in-cell crowding," *Proc. Natl. Acad. Sci. U. S. A.*, 2016, **113**,1684-1685, and references therein.

5 D. S. Goodsell, Biochem. "Miniseries: Illustrating the Machinery of Life: *Escherichia coli*," *Mol. Biol. Educ.*, 2009, **37**, 325-332.

6 K. A. Sharp, "Analysis of the size dependence of macromolecular crowding shows that smaller is better," *Proc. Natl. Acad. Sci. U. S. A.*, 2015, **112**, 7990-7995.

7 J. Pelletier, K. Halvorsen, B. Y. Ha, R. Paparcone, S. J. Sandler, C. L. Woldringh, W. P. Wong, and S. Jun, "Physical manipulation of the *Escherichia coli* chromosome reveals its soft nature," *Proc. Natl. Acad. Sci. U. S. A.*, 2012, **109**, E2649-E2656.

8 H. X. Zhou, "Influence of crowded cellular environments on protein folding, binding, and oligomerization: Biological consequences and potentials of atomistic modeling," *FEBS Lett.* 2013, **587**, 1053-1061.

9 S. Jun, "Chromosome, Cell Cycle, and Entropy," *Biophys. J.* **108**, 2015, 785-786.

10 D. Marenduzzo, C. Micheletti, and P. R. Cook, "Entropy-Driven Genome Organization," *Biophys. J.*, 2006, **90**, 3712-3721.

11 D. Marenduzzo, I. Faro-Trindade, and P. R. Cook, "What are the molecular ties that maintain genomic loops?" *TRENDS in Genetics*, 2007, **23**, 126-133.

12 S. Asakura and F. Oosawa, "On Interaction between Two Bodies Immersed in a Solution of Macromolecules," *J. Chem. Phys.*, 1954, **22**, 1255-1256.

13 H. N. W. Lekkerkerker and R. Tuinier, "Colloids and the Depletion Interaction," *Lecture Notes in Physics* **833** (Springer 2011).

14 J. A. Valkenburg and C. L. Woldringh, "Phase Separation Between Nucleoid and Cytoplasm in *Escherichia coli* as Defined by Immersive Refractometry," *J. Bacteriol.*, 1984, **160**, 1151-1157.

15 C. L. Woldringh and T. Odijk in *Organization of the Prokaryotic Genome*, ed. R. L. Charlebois, ASM Press (Washington, D.C., 1999).

16 J. Stavans and A. Oppenheim, "DNA-protein interactions and bacterial chromosome architecture," *Phys. Biol.*, 2006, **3**, R1-R10.

17 H. Kang, P. A. Pincus, C. Hyeon, and D. Thirumalai, "Effects of Macromolecular Crowding on the Collapse of Biopolymers," *Phys. Rev. Lett.*, 2015, **114**, 068303–1-5.

18 C. Jeon et al, *Soft Matter*, 2016, DOI: 10.1039/C6SM01184E.

19 F. C. Neidhardt, J. L. Ingraham, and M. Schaechter, *Physiology of the Bacterial Cell: A Molecular Approach* (Sinauer Associates, 1990).

20 H. Bremer and P. Dennis, "Modulation of Chemical Composition and Other Parameters of the Cell by Growth Rate" in *Escherichia coli and Salmonella: Cellular and Molecular Biology*," ed. F. C. Neidhardt (ASM Press, 1996).

21 O. L. Miller, Jr., Barbara A. Hamkalo and C. A. Thomas, Jr., "Visualization of Bacterial Genes in Action," *Science*, New Series, 1970, **169**, 392-395.

22 S. L. French and O. L. Miller, Jr, "Transcription mapping of the Escherichia coli chromosome by electron microscopy," *J. Bacteriol.*, 1989, **171**, 4207-4216.

23 J. Kim, C. Jeon, H. Jeong, Y. Jung, and B.-Y. Ha, "A polymer in a crowded and confined space: effects of crowder size and poly-dispersity," *Soft Matter*, 2015, **11**, 1877-1888.

24 T. N. Shendruk, M. Bertrand, H. W. de Haan, J. L. Harden, and G. W. Slater, "Simulating the Entropic Collapse of Coarse-Grained Chromosomes," *Biophys. J.*, 2015, **108**, 810-820.

25 T. N. Shendruk, M. Bertrand, J. L. Harden, G. W. Slater, and H. W. de Haan, "Coarse-grained molecular dynamics simulations of depletion-induced interactions for soft matter systems," *J. Chem. Phys.*, 2014, **141**, 244910–1-11.

26 J. J. Jones, J. R. C. van der Maarel, and P. S. Doyle, "Effect of Nanochannel Geometry on DNA Structure in the Presence of Macromolecular Crowding Agent," *Nano Lett.*, 2011, **11**, 5047-5053.

27 B.-Y. Ha and Y. Jung, "Polymers under confinement: single polymers, how they interact, and as model chromosomes," *Soft Matter*, 2015, **11**, 2333-2352.

28 B. Youngren, H. J. Nielsen, S. Jun, and S. Austin, "The multifork Escherichia coli chromosome is a self-duplicating and self-segregating thermodynamic ring polymer," *Genes Dev.*, 2014, **28**, 71-84.

29 X. Wang, P. M. Llopis, and D. Z. Rudner, "Organization and segregation of bacterial chromosomes," *Nat. Rev. Genetics*, 2013, **14**, 191-203.

30 C. Jeon, J. Kim, H. Jeong, Y. Jung, and B.-Y. Ha, "Chromosome-like organization of an asymmetrical ring polymer confined in a cylindrical space," *Soft Matter*, 2015, **11**, 8179-8193.

31 P. R. Cook and D. Marenduzzo, "Entropic organization of interphase chromosomes," *J. Cell Biol.*, 2009, **186**, 825-834.

32 J. Shin, A. G. Cherstvy, and R. Metzler, "Mixing and segregation of ring polymers: spatial confinement and molecular crowding effects," *New J. Phys.*, 2014, **16**, 053047–1-19.

33 M. Rubinstein and R. H. Colby, *Polymer Physics* (Oxford University Press, 2003).

34 R. de Vries, "Flexible Polymer-Induced Condensation and Bundle Formation of DNA and F-Actin Filaments," *Biophys. J.*, 2001, **80**, 1186-1194.

35 J. D. Weeks, D. Chandler and H. C. Andersen, "Role of Repulsive Forces in Determining the Equilibrium Structure of Simple Liquids," *J. Chem. Phys.*, 1971, **54**, 5237-5247.

36 K. Kremer and G. S. Grest, "Dynamics of entangled linear polymer melts- A molecular-dynamics simulation," *J. Chem. Phys.*, 1990, **92**, 5057- 5086.

37 G. S. Grest and K. Kremer, "Molecular dynamics simulation for polymers in the presence of a heat bath," *Phys. Rev. A*, 1986, **33**, R3628-R3631.

38 M. P. Allen and D. J. Tildesley, *Computer Simulation of Liquids* (Clarendon, Oxford, 1987).

39 Y. Jung, C. Jeon, J. Kim, H. Jeong, S. Jun, and B.-Y. Ha, "Ring polymers as model bacterial chromosomes: confinement, chain topology, single chain statistics, and how they interact," *Soft Matter*, 2012, **8**, 2095-2102.

40 A. Grosberg and A. R. Khokhlov, *Statistical Physics of Macromolecules* (AIP Press, New York, 1994).

41 M. Dijkstra, R. van Roij, and R. Evans, "Phase diagram of highly asymmetric binary hard-sphere mixtures," *Phys. Rev. E*, 1999, **59**, 5744-5771.

42 M. Doi, *Soft Matter Physics* (Oxford University Press, 2013).

43 K. A. Dill and S. Bromberg, *Molecular Driving Forces: Statistical Thermodynamics in Biology, Chemistry, Physics, and Nanoscience*, 2nd Edt. (Garland Science, 2012).

44 C. Jeon, *private communication*, 2016.

45 S. Jun, J. Bechhoefer, and B.-Y. Ha, "Diffusion-limited loop formation of semiflexible polymers: Kramers theory and the intertwined time scales of chain relaxation and closing," *Europhys. Lett.*, 2003, **64**, 420-426.

46 D. J. Jin and J. E. Cabrera, "Coupling the distribution of RNA polymerase to global gene regulation and the dynamic structure of the bacterial nucleoid in *Escherichia coli*," *J. Struct. Biol.*, 2006, **156**, 284-291.

47 D. J. Jin, C. Cagliero, and Y. N. Zhou, "Role of RNA Polymerase and Transcription in the Organization of the Bacterial Nucleoid." *Chem. Rev.*, 2013, **113**, 8662-8682.

48 U. Endesfelder, K. Finan, S. J. Holden, P. R. Cook, A. N. Kapanidis, and M. Heilemann, "Multiscale Spatial Organization of RNA Polymerase in *Escherichia coli*," *Biophys. J.*, 2013, **105**, 172-181.

49 R. Milo and R. Phillips, *Cell Biology by the Numbers* (Garland Science, 2015).

50 R. Phillips, J. Kondev, J. Theriot, and H. Garcia, *Physical Biology of the Cell*, 2nd Edt. (Garland Science, 2012).

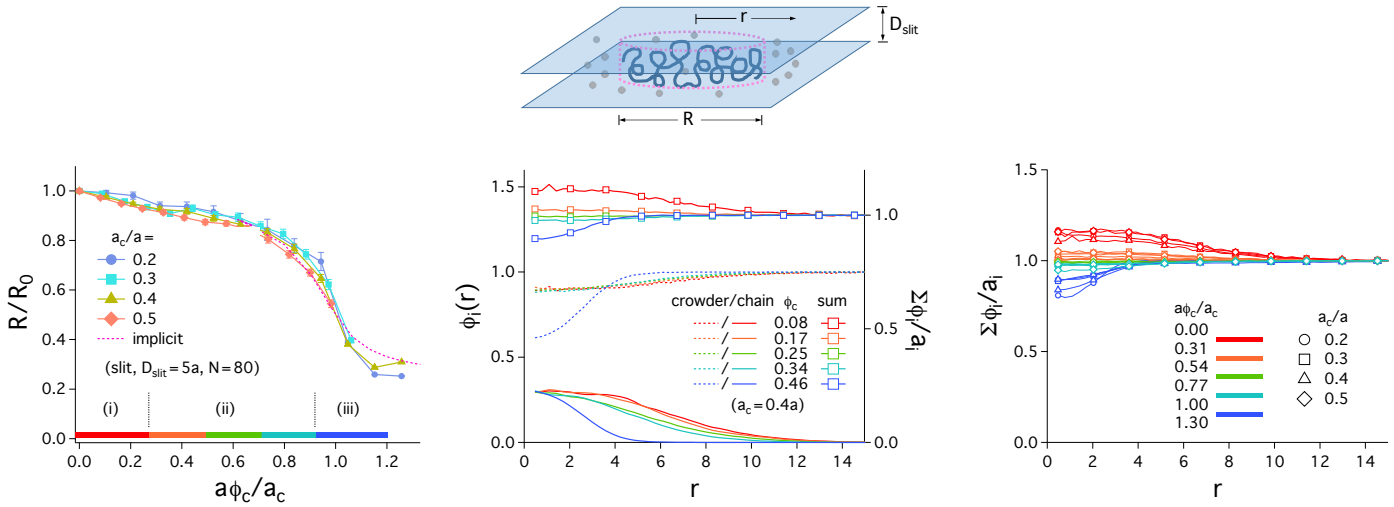

Fig. 4 Reduction of polymer size by molecular crowding (left) and spatial distribution of monomers and crowders (middle and right) in a quasi-two-dimensional slit-like space for the case $a > a_c$. The simulation parameters used are $N = 80$, the slit gap $D_{\rm slit} = 5a$, and $a_c = 0.2, 0.3, 0.4, 0.5a$. In the left graph, the normalized chain size R/R_0 is plotted against the ratio ϕ_c/a_c, where R_0 is the equilibrium chain size in the absence of crowders and $\phi_c = \phi_c(r = \infty)$. The ratio R/R_0 is a function of ϕ_c/a_c for $a > a_c$. The dashed line in magenta is the result obtained by mapping the explicit-crowder case onto an effective-solvent picture, in which the effects of crowders are mimicked by reducing the excluded volume of monomers v [18]. The varying degrees of compaction is represented by the color bar on the x axis: weak (i), moderate (ii), and strong (iii); the color bar matches the color scheme used in the other two graphs. In the middle graph, the volume fraction $\phi_i(r)$ of monomers and crowders with $i =$ 'm' (monomer) or 'c' (crowder) is plotted on the left axis, and $\sum_i \phi_i(r)/a_i$ on the right axis, for $a_c = 0.4a$; also note that r is the longitudinal distance from the center of mass of the polymer. For visual clarity, $\phi_c(r)$ is normalized as $\phi_c(r)/\phi_c(r = \infty)$ and $\phi_m(r)$ as $\phi_m(r)/\phi_m(r = 0)$; $\sum_i \phi_i(r)/a_i$ is rescaled by $\sum_i \phi_i(r = \infty)/a_i$. Consistent with the results for a free space in Fig. 2, in regime (ii), $\sum_i \phi_i(r)/a_i$ tends to a constant through the entire range of r shown and converges onto $\phi_c(r = \infty)/a_c$. The graph on the right summarizes the results for $\sum_i \phi_i(r)/a_i$ for various choices of a_c. In regime (ii), $\sum_i \phi_i(r)/a_i \approx \phi_c(r = \infty)/a_c$ is satisfied for all a_c values used. Outside regime (ii), $\sum_i \phi(r)/a_i$ deviates a bit more appreciably from $\sum_i \phi_i(r = \infty)/a_i$ (up to 15%). As noted earlier (Fig. 2), the sum rule is invariant under the exchange in role between monomers and crowders. (Error bars are shown for a few representative curves.)

Appendix

In this Appendix, we justify the sum rule in Eq. 5 for confined cases. First note that it is a local relation. Unlike large scale properties, the way monomers and crowders are spatially distributed at a given position is expected to be insensitive to confinement, as demonstrated here.

Fig. 4 displays our results for chain compaction and spatial organization of monomers and crowders for a quasi-two-dimensional slit-like space. The simulation parameters used are $N = 80$, $D_{\rm slit} = 5a$, and $a_c = 0.2, 0.3, 0.4, 0.5a$ ($a > a_c$). These results can readily be understood in parallel with those in Fig. 2.

First, the graph on the left suggests that normalized chain size R/R_0 is a function of the ratio $a\phi_c/a_c$, similarly to what is seen in the corresponding unconfined case in Fig. 2; recall that R_0 is the equilibrium chain size in the absence of crowders. Also shown is an effective-solvent result (dashed line in magenta) obtained in the same way discussed in subsec. 3.1. The color bar on the x axis represents a varying degree of compaction: weak (i), moderate (ii), and strong (iii); it matches the color scheme used in the other two graphs.

The middle graph shows the volume fraction $\phi_i(r)$ of monomers and crowders with $i =$ 'm' (monomer) or 'c' (crowder) plotted on the left axis as well as $\sum_i \phi_i(r)/a_i$ on the right axis, for $a_c = 0.4a$; here, r is the longitudinal distance from the center of mass of the polymer. For visual clarity, $\phi_c(r)$ is normalized as $\phi_c(r)/\phi_c(r = \infty)$ and $\phi_m(r)$ as $\phi_m(r)/\phi_m(r = 0)$; $\sum \phi_i(r)/a_i$ is rescaled by $\sum_i \phi_i(r = \infty)/a_i$. Consistent with the results for a free space in Fig. 2, in regime (ii), $\sum_i \phi_i(r)/a_i$ tends to a constant through the entire range of r shown and converges onto $\phi_c(r = \infty)/a_c$.

The results for $\sum_i \phi_i(r)/a_i$ for various choices of a_c are displayed in the graph on the right. In accord with what is shown in the graph on the right for $a > a_c$ in Fig. 2, in regime (ii), $\sum_i \phi_i(r)/a_i \approx \phi_c(r = \infty)/a_c$ is satisfied for all a_c values used:

$$\frac{\phi(r)}{a} + \frac{\phi_c(r)}{a_c} \approx \frac{\phi_c(r = \infty)}{a_c} = \frac{\phi_c}{a_c} \qquad \text{(slit)}. \qquad (14)$$

Outside regime (ii), $\sum_i \phi(r)/a_i$ deviates a bit more appreciably from $\sum \phi_i(r = \infty)/a_i$ (up to 15%).

Fig. 2 suggests that the sum rule holds for both $a > a_c$ and $a < a_c$. In our view, this is a natural consequence of the functional form of Eq. 5: the terms on the left hand side is symmetric with respect to the exchange between the roles of a and a_c. By the same token, we argue that the sum rule in Eq. 14 works for $a_c > a$. For a reason similar to the one describe earlier in the Appendix (i.e., locality of $\phi_i(r)$), it is expected to hold for a cylindrically confined case (data not shown).

TOC Graphic

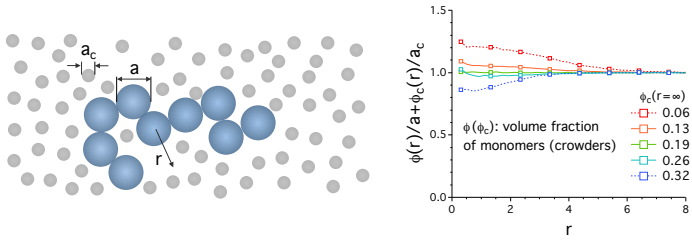

Fig. 5 Interrelationship between molecular crowding and the spatial organization of a biopolymer: the sum of the volume fractions of monomers and crowders rescaled by their size is constant in a parameter space of biophysical interest (the data are normalized at $r = \infty$).